

Article

Characterization of a Metallic-Ions-Independent L-Arabinose Isomerase from Endophytic *Bacillus amyloliquefaciens* for Production of D-Tagatose as a Functional Sweetener

Hoda M. Shehata¹, Mohamed N. Abd El-Ghany^{1,*}, Salwa A. Hamdi², Mosleh M. Abomughaid³,
Khaled I. Ghaleb³, Zeinat Kamel¹ and Mohamed G. Farahat^{1,4,*}

¹ Botany and Microbiology Department, Faculty of Science, Cairo University, Giza 12613, Egypt; hodashehata@sci.cu.edu.eg (H.M.S.)

² Zoology Department, Faculty of Science, Cairo University, Giza 12613, Egypt

³ Medical Laboratory Sciences Department, College of Applied Medical Sciences, University of Bisha, Bisha 67714, Saudi Arabia

⁴ Biotechnology Department, Faculty of Nanotechnology for Postgraduate Studies, Cairo University, Sheikh Zayed Branch Campus, Giza 12588, Egypt

* Correspondence: mabdelghany@sci.cu.edu.eg (M.N.A.E.-G.); farahat@cu.edu.eg (M.G.F.)

Abstract: D-Tagatose is a low-calorie sugar substitute that has gained increased attention as a functional sweetener owing to its nutraceutical and prebiotic properties. Traditionally, D-tagatose is produced via the enzymatic conversion of L-galactose to D-tagatose by L-arabinose isomerase (L-AI). Nonetheless, the most reported L-AI enzymes are ion-dependent enzymes requiring Mn^{2+} and/or Co^{2+} as cofactors for their reactions, which limits their application due to safety and health concerns. Herein, we addressed the facile bioconversion of L-galactose to D-tagatose using a novel recombinant metallic-ions-independent L-AI derived from endophytic *Bacillus amyloliquefaciens* CAAI isolated from cantaloupe fruits. The ORF (1500 bp) of the L-arabinose isomerase gene (*araA*) was cloned and over-expressed in *Escherichia coli*. The recombinant enzyme (BAAI) was purified to homogeneity using Ni-NTA affinity chromatography, yielding a single distinct band with an apparent molecular mass of approximately 59 kDa as deduced from SDS-PAGE analysis. The purified enzyme showed optimum activity at pH and temperature of 7.5 and 45 °C, respectively, with obvious enzymatic activity in the presence of ethylenediaminetetraacetic acid (EDTA), indicating the metallic-ions independence from BAAI. The K_m values of BAAI for D-galactose and L-arabinose were 251.6 mM and 92.8 mM, respectively. The catalytic efficiency (k_{cat}/K_m) values for D-galactose and L-arabinose were found to be 2.34 and 46.85 $mM^{-1} min^{-1}$, respectively. The results revealed the production of 47.2 g/L D-tagatose from D-galactose (100 g/L) with 47.2% bioconversion efficiency in a metallic-ions-free reaction system that could be implemented in safe-production of food-grade low-calorie sweetener, D-tagatose.

Keywords: L-arabinose isomerase; tagatose production; recombinant enzyme; enzyme characterization; endophytic bacteria; *Bacillus amyloliquefaciens*



Citation: Shehata, H.M.; Abd El-Ghany, M.N.; Hamdi, S.A.; Abomughaid, M.M.; Ghaleb, K.I.; Kamel, Z.; Farahat, M.G. Characterization of a Metallic-Ions-Independent L-Arabinose Isomerase from Endophytic *Bacillus amyloliquefaciens* for Production of D-Tagatose as a Functional Sweetener. *Fermentation* **2023**, *9*, 749. <https://doi.org/10.3390/fermentation9080749>

Academic Editors: Guoqiang Zhang and Jianghua Li

Received: 13 July 2023

Revised: 8 August 2023

Accepted: 11 August 2023

Published: 12 August 2023



Copyright: © 2023 by the authors. Licensee MDPI, Basel, Switzerland. This article is an open access article distributed under the terms and conditions of the Creative Commons Attribution (CC BY) license (<https://creativecommons.org/licenses/by/4.0/>).

1. Introduction

D-Tagatose is a rare monosaccharide that recently occupies a significant niche among emerging low-calorie sweeteners. It has been considered a potential replacement for sucrose due to its low calorific value and resemblance to sucrose taste, with no cooling effect, aftertaste, or potentiation of off-flavors [1–4]. D-Tagatose has a relative sweetness value of 92% when compared with sucrose, with a low glycemic effect [1]. Thus, it has many benefits for human health as the control of type II diabetes, obesity [2,5–7], and hyperglycemia [8,9]. In addition, it reduces dental caries [10] and has appropriate improvements in HDL and total cholesterol [5,11,12]. Furthermore, D-tagatose has antioxidant activity as a free radical

trapper [13] and has cytoprotective [14,15] and prebiotic effects [16,17]. Recently, D-tagatose was found to protect against oleic acid-induced acute respiratory distress syndrome [18]. Additionally, D-tagatose has recently been identified as a potential nutraceutical [19]. Besides its health benefits, D-tagatose inhibits the growth of various phytopathogens with negligible adverse effects on human health, suggesting its potential use as an eco-friendly alternative to fungicides in crop protection [20]. In a recent study, D-tagatose has been documented to trigger sweet immunity and resistance of grapevine to downy mildew caused by *Plasmopara viticola* [21]. Moreover, it suppresses the late blight of tomato caused by *Phytophthora infestans* [22]. It has been suggested that applications of D-tagatose could be a novel strategy for cucumber protection against powdery mildew caused by *Podosphaera xanthii* via the direct inhibition of conidial germination [23]. Furthermore, D-tagatose is an intermediate chemical to synthesize various valuable compounds such as texturizers, detergents, stabilizers, and humectants in cosmetics and toothpaste [24].

D-Tagatose occurs naturally as a rare hexose in the gum exudate of the cacao tree (*Sterculia setigera*) and in tiny amounts of a few plant species [25]. However, it can be produced from D-galactose via either chemical synthesis or biological-mediated methods [26]. The chemical synthesis approach involves the direct isomerization of D-galactose using metal hydroxides; however, the drastic reaction conditions and high cost of the subsequent purification steps are the major drawbacks of this method [27]. In recent years, biological manufacturing of D-tagatose using L-arabinose isomerase (L-AI) has been intensively studied to resolve the disadvantages of the chemical methods. In this context, L-AI (EC 5.3.1.4) is an intracellular enzyme that catalyzes the reversible isomerization of L-arabinose to L-ribulose as well as D-galactose to D-tagatose (Figure 1), based on similarity in the substrate configuration [3,28,29]. This enzyme is expected to become the second aldose isomerase that has many industrial applications following the D-xylose isomerase [30]. Owing to their rarity in nature and their costly processing processes, isomerase enzymes are becoming particularly important because they play a crucial role in the synthesis of rare sugars. In this trend, several L-AIs have been discovered and characterized from different microorganisms to be used for D-tagatose biosynthesis. Hitherto, numerous microbial species were found to produce L-AI including such as *Lactobacillus fermentum* [31], *Lactobacillus sakai* 23 K [32], *Klebsiella pneumoniae* [33], *Lactococcus lactis* [34], *Bacillus subtilis* [35], *Shewanella* sp. [36], *Enterococcus faecium* [37], *Clostridium hylemonae* [26], *Alicyclobacillus hesperidum* URH17-3-68 [38], *Anoxybacillus flavithermus* [39], *Arthrobacter* sp. 22c [40], *Bacillus thermoglucosidasius* KCTC 1828 [41], *Geobacillus stearothermophilus* [42], *Lactobacillus plantarum* [43], *Pediococcus pentosaceus* PC-5 [44], *Pseudoalteromonas haloplanktis* ATCC 14,393 [45] and *Shigella flexneri* [46]. However, the vast majority of the reported L-AIs have been found to depend on Mn^{2+} and/or Co^{2+} for their catalytic reactions. Thus, the exploration of new sources of ion-independent L-AI is of great interest in food applications. Herein, we report for the first time on the expression, characterization, and application of a novel metallic-ions-independent L-AI from the endophytic bacterium *Bacillus amyloliquefaciens* CAAI for the efficient bioconversion of D-galactose to D-tagatose.

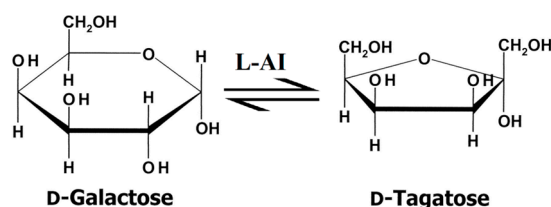


Figure 1. Isomerization reaction of D-galactose to D-tagatose catalyzed by L-AI.

2. Materials and Methods

2.1. Isolation of Endophytic Bacteria

Healthy and undamaged cantaloupe fruits were bought from local markets and washed under running water. Afterward, the collected plant samples were surface sterilized

to eliminate epiphytes by immersing them in 0.1% mercuric chloride for 2 min, 75% ethanol for 2 min, and 5% sodium hypochlorite for 5 min, respectively. Then, surface-sterilized plant samples were washed several times with sterile distilled water and cut into small pieces and squeezed in a sterile mortar and pestle with 50 mM phosphate buffer (pH 7.5). Then, each extract was serially diluted, and 0.1 mL of the aliquots were spread on modified M9 agar (Bio Basic, Markham, ON, Canada) containing 1% D-galactose as the sole carbon source. The inoculated plates were incubated for 24–48 h at 37 °C. Then, single bacterial colonies were picked and purified.

2.2. Screening and Identification of L-Arabinose Isomerase-Producing Bacteria

The isolated endophytes were screened for intracellular L-AI activity. Briefly, each isolate was inoculated into a modified M9 broth containing 1% L-galactose as the sole carbon source and incubated at 37 °C for 48 h with shaking (150 rpm). Subsequently, cells were harvested via centrifugation at $10,000 \times g$ for 10 min at 4 °C. The collected cells were washed three times with sterile saline, resuspended in 50 mM Tris-HCl buffer (pH 7.5), and disrupted via sonication for 6 cycles (10 s bursts at 200 Watt with a 10 s pause period after each burst). The cell lysates were centrifuged at $20,000 \times g$ for 10 min at 4 °C, and the supernatants were assayed for L-AI activity. The reaction mixture contained 1 mM $MnCl_2$, 500 mM D-galactose, 200 μ L of cell-free extract, and 50 mM Tris-HCl buffer (pH 7.5) to bring the final volume to 1 mL. The assay was performed by incubating the reaction mixture and enzyme at 50 °C for 1 h. Subsequently, the enzymatic reaction was stopped by cooling the samples on ice. The produced D-tagatose was determined following the cysteine carbazole sulfuric acid method [47]. In another set, metallic-ions-independent L-AI enzymes were screened using the same method, but the enzyme assay was performed in the presence of 1 mM EDTA without the incorporation of $MnCl_2$. Based on the screening results, a promising strain that produced a metallic-ions-independent L-AI was selected and identified according to its 16S rRNA gene sequence as described elsewhere [48].

2.3. Cloning and Sequence Analysis of L-Arabinose Isomerase Gene

The amplification of the L-AI gene (*araA*) gene from *B. amyloliquefaciens* CAAI was conducted through the polymerase chain reaction (PCR) using the Phusion High-Fidelity DNA polymerase (Thermo Scientific, MA, USA). In this study, the forward (5'-ACTGGATCCATG AATGTGCTTCAGAACAAG-3') and reverse (5'-ACGAAGCTTTCAAATCCCTCCCAAC-3') primers were designed based on the sequence of the open reading frame (ORF) published in GenBank (*B. amyloliquefaciens* DSM7; Accession number FN597644.1, REGION: c2736257-2734758). The BamHI and HindIII restriction sites (underlined) were incorporated into the primers at their 5' ends, respectively. The PCR contained 10 μ L 5X Phusion Green HF buffer, 200 μ M dNTPs, 0.4 μ M of each primer, 1 μ g genomic DNA template, one Unit of the Phusion DNA polymerase (Thermo Scientific, Waltham, MA, USA) and nuclease-free water to make volume up to 50 μ L. The PCR was conducted in a ProFlex thermocycler (Applied Biosystems, Foster City, CA, USA) using the following program: initial denaturation at 98 °C for 30 s, followed by 30 cycles of denaturation at 98 °C for 10 s, annealing at 68.4 °C for 30 s, extension at 72 °C for 50 s, and a final extension at 72 °C for 10 min. After checking the quality and integrity of the amplicons by agarose gel electrophoresis, bands of the expected size were excised with clean, sharp scalpels and eluted by using the QIAquick Gel Extraction Kit (Qiagen, Hilden, Germany) according to the manufacturer's protocol. Afterward, the PCR product and pQE-80L-kan expression vector were digested by BamHI and HindIII restriction enzymes (FastDigest, Thermo Scientific, USA), gel-purified, and ligated using T4 DNA ligase (Thermo Scientific, USA). After the transformation into *E. coli* BL21 (DE3) using a TransformAid bacterial transformation kit (Thermo Scientific, USA), the transformed cells were selected on LB agar supplemented with kanamycin (25 μ g/mL). Finally, the recombinant plasmids were extracted from overnight cultures using GeneJET Plasmid Miniprep Kit (Thermo Scientific, USA) and sequenced. The BLAST analysis was conducted by submitting the nucleotide and the deduced amino acid sequences to the NCBI

BLAST server (<http://blast.ncbi.nlm.nih.gov/Blast.cgi>, accessed on 20 June 2023). Multiple amino acid sequence alignment analysis was accomplished using the Clustalw online tool (<https://www.genome.jp/tools-bin/clustalw>, accessed on 20 June 2023) and visualized using CLC main workbench software (version 6.5). The InterProScan tool was used for the classification and characterization of the protein [49]. The ProtParam tool was used for computing the physicochemical properties of the deduced amino acid sequence [50]. The structural model of L-AI derived from *B. amyloliquefaciens* CAAI was generated via homology modeling using SWISS-MODEL (<http://swissmodel.expasy.org/>, accessed on 24 July 2023). The metal-binding sites of the generated model were checked using the AlphaFold protein structure database (<https://alphafold.ebi.ac.uk/>, accessed on 24 July 2023), and the predicted structure was visualized using Pymol software (version 2.0.7). The presence of disulfide bonds was predicted using the Dipro tool (<http://scratch.proteomics.ics.uci.edu/>, accessed on 24 July 2023).

2.4. Expression and Characterization of L-Arabinose Isomerase

To express the recombinant L-AI derived from *B. amyloliquefaciens* CAAI, the *E. coli* BL21 (DE3) harboring the recombinant plasmid was cultured in LB broth supplemented with kanamycin (25 µg/mL) in a shaking incubator (180 rpm) at 37 °C until an OD_{600nm} of 0.6 is reached. Subsequently, isopropylthio-β-galactoside (IPTG) was added at a final concentration of 1 mM to induce the protein expression at 37 °C for 4 h. Thereafter, the induced cells were harvested via centrifugation at 8000× g for 10 min at 4 °C and resuspended in a lysis buffer containing lysozyme (1 mg/mL) and incubated on ice for 30 min. Afterward, the induced cells were disrupted via ultrasonication (30 s pulse on and 10 s pulse off) on ice for 10 min. After centrifugation (20,000× g, 5 min) at 4 °C, the supernatant was loaded onto the Ni-NTA superflow column (Qiagen, Hilden, Germany), and the His₆-tagged enzyme was purified as described elsewhere [51]. Finally, the eluted His₆-tagged enzyme (referred to as BAAI) was dialyzed against 50 mM Tris-HCl buffer (pH 7.5) at 4 °C with several buffer exchanges for 24 h. The purity of the recombinant BAAI was checked by 12% SDS-PAGE and visualized via staining with Coomassie blue R250.

2.5. Characterization of BAAI

The L-AI activity of BAAI was assayed by determining the amount of D-tagatose from the isomerization of D-galactose, as described above. One unit (U) of L-AI activity was defined as the amount of enzyme that catalyzes the formation 1 µmol D-tagatose per min at the reaction conditions. The concentration of the produced D-tagatose was estimated based on the standard linear graph prepared using different concentrations of D-tagatose. The protein concentration was estimated according to Bradford's method with bovine serum albumin (Sigma Aldrich) as a standard [52]. The optimum temperature of BAAI was determined by conducting the enzyme assay at various temperatures (20–70 °C). The enzyme activity at the optimum temperature was considered to be 100%. The optimal pH of BAAI was investigated by assaying its activity in 50 mM of different buffer systems within pH 3.0–13.0. To achieve various pH values, seven buffer systems were used: glycine-HCl (pH 3.0), sodium acetate buffer (pH 4.0–5.0), phosphate buffer (6.0 to 7.5), Tris-HCl buffer (pH 8.0–9.0), glycine-NaOH (pH 10.0), monosodium phosphate-NaOH (pH 11.0), and potassium chloride-NaOH (pH 12.0–13.0). The quantity of D-tagatose obtained from D-galactose was then determined calorimetrically, and relative activity was determined. The enzyme activity at the optimum pH was considered 100%. To evaluate the effect of metallic ions on the thermal stability and activity of BAAI, the purified enzyme was first dialyzed against a 50 mM Tris-HCl buffer (pH 7.5) containing 10 mM EDTA for 24 h at 4 °C (to make it metal-free). Subsequently, the enzyme was dialyzed against 50 mM EDTA-free Tris-HCl buffer (pH 7.5) for 24 h at 4 °C. The thermal stability of BAAI was investigated via the pre-incubation of the enzyme and the metal-free enzyme at different temperatures for 120 min before the measurement of the residual activities. The enzymatic activity of BAAI and EDTA-treated BAAI that pre-incubated on ice for the same time represents 100%. To

assess the effect of various metal ions, the enzyme activity was measured at the optimum temperature and pH for 30 min in the presence of one specific divalent metal ion (Pb^{2+} , Cr^{2+} , Cu^{2+} , Zn^{2+} , Ba^{2+} , Sn^{2+} , Mg^{2+} , Ca^{2+} , Hg^{2+} , Mn^{2+} , and Co^{2+}) with a final concentration of 1 mM. The enzyme activity was determined by using the same enzyme assay (as described above). The activity of the enzyme was defined as the value relative to its activity without metal ions (the enzymatic activity without any metal ion addition was taken as 100%). In addition to the treatment with EDTA, the metal-free enzyme was prepared via dialysis against 50 mM Tris-HCl buffer (pH 7.5) containing 1,10-phenanthroline (10 mM) as a chelating agent for 24 h at 4 °C. After dialysis against five changes of 50 mM Tris-HCl buffer (pH 7.5), the enzyme activity was assayed. Enzyme kinetics parameters of BAAI were determined by assaying the enzyme with various concentrations of D-galactose and L-arabinose. The Michaelis–Menten constant (K_m), maximum velocity (V_{\max}), turnover numbers (k_{cat}) and catalytic efficiencies (k_{cat}/K_m) were calculated via nonlinear regression using GraphPad Prism software (Version 9.5.1).

2.6. Bioconversion of D-Galactose into D-Tagatose by BAAI

To investigate the bioconversion catalytic potential of BAAI, the purified recombinant enzyme (50 U) was added to 100 mL of D-galactose solution (100 g/L) in 50 mM Tris-HCl buffer (pH 7.5), and the reaction was incubated at 45 °C for 24 h. Subsequently, the produced D-tagatose was determined. The bioconversion yield was calculated as the ratio between the concentrations of D-tagatose (product) and the initial concentration of D-galactose (substrate).

2.7. Statistical Analysis

All mentioned experiments were performed in triplicates, and the obtained data are presented as the mean \pm standard deviation (SD). The statistical significance of differences was determined using analysis of variance (ANOVA) and Post hoc with multiple comparison tests using Duncan's method, where differences at p -value < 0.05 were considered significant. All statistical analyses were conducted using the IBM SPSS software version 22.

3. Results

3.1. Isolation and Identification of L-Arabinose Isomerase-Producing Bacteria

Thirty-eight endophytic bacterial isolates were recovered from cantaloupe fruits using the modified M9 agar containing 1% D-galactose as the sole carbon source. The results revealed that 14 endophytic isolates exhibited L-AI activity in the presence of Mn^{2+} . Of all investigated endophytes, only one isolate (designated CAAI) showed L-AI activity in the presence of EDTA, indicating its ion-independency catalytic activity. Accordingly, the CAAI endophytic bacterial isolate was selected for further investigations. The selected isolate was identified based on its 16S rRNA gene sequence. The phylogenetic analysis revealed that the bacterial isolate CAAI was identified as *Bacillus amyloliquefaciens*. BLAST results indicated that *B. amyloliquefaciens* strain CAAI shares 99.85% similarity with *B. amyloliquefaciens* strain BCRC 11601 (Accession number: NR_116022.1), 99.62% with *Bacillus vallismortis* strain DSM 11031 (Accession number: NR_024696.1) and 99.55% with *Bacillus vallismortis* strain NBRC 101236 (Accession number: NR_113994.1). The 16S rRNA gene sequence of *B. amyloliquefaciens* CAAI (1333 bp) was submitted to the GenBank under the accession number MK389270.1, and the neighbor-joining phylogenetic tree was constructed (Figure 2).

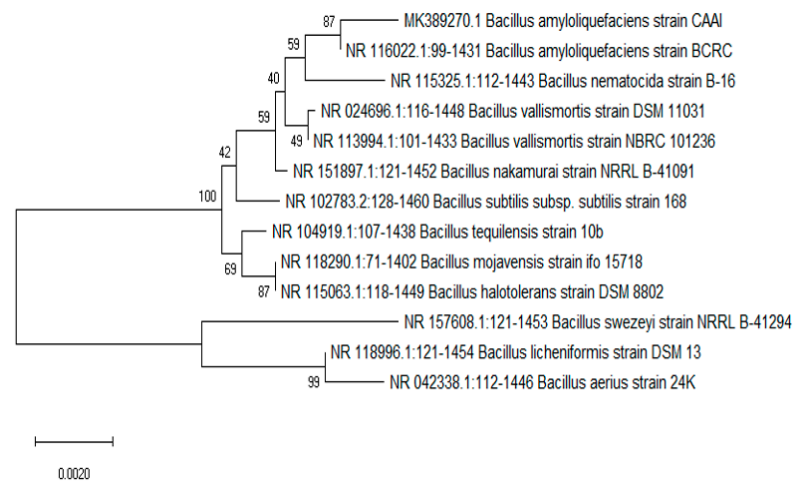


Figure 2. Neighbor-joining phylogenetic tree based on 16S rRNA gene sequences showing the relationship between *B. amyloliquefaciens* CAAI and the most closely related species.

3.2. Cloning and Sequence Analysis

The putative L-AI gene (*araA*) of *B. amyloliquefaciens* was amplified via PCR, and the amplicon was checked via agarose gel electrophoresis (Figure 3). The results revealed the amplification of a 1500 bp fragment corresponding to the open reading frame (ORFs) of the *araA* of *B. amyloliquefaciens*.

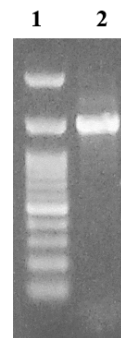


Figure 3. Agarose gel electrophoresis of a PCR amplified of putative *araA* gene amplified from the genomic DNA of *B. amyloliquefaciens* CAAI. Lane 1, DNA marker; lane 2, PCR amplicon of the putative *araA* gene (1500 bp).

Then, the putative gene was ligated into a pQE-80L-Kan expression vector under the control of a T5 promoter and in frame with the N-terminal region coding for six histidine residues to accelerate the protein purification process. Following ligation, the recombinant plasmid was transformed into *E. coli* BL21. The nucleotide sequences of the putative genes *araA* gene of *B. amyloliquefaciens* strain CAAI was submitted to the NCBI database, and an accession number MK393916.1 was assigned. The results revealed that the sequence of the putative *araA* gene of *B. amyloliquefaciens* consisted of 1500 bp and coding for 499 amino acid residues. BLASTp analysis showed that the deduced amino acid sequence of *araA* gene of *B. amyloliquefaciens* (accession number: QBY21424.1) shared 100% identity with the L-AI of *B. amyloliquefaciens* (accession number: KYC93437.1), 97.39% identity with the L-AI of *Bacillus velezensis* (accession number: WP_014418599.1), 96.79% identity with the L-AI of *Bacillus siamensis* (accession number: OAZ69248.1) and 84.62% identity with the L-AI of *Bacillus halotolerans* (accession number: WP_069487080.1). The multiple sequence alignments of the deduced amino acid sequence with other bacterial L-AIs displayed the conserved residues across the species (Figure 4). The physicochemical properties obtained from ProtParam analysis were tabulated (Table 1). The molecular weight of the deduced amino acid sequence was estimated to be 56.41 kDa. The predicted instability index and

theoretical isoelectric point (pI) values were 35.77 and 5.45, respectively. Furthermore, ProtParam results revealed the presence of 70 negatively charged and 52 positively charged residues. Additionally, the grand average of hydropathicity (GRAVY) and aliphatic index were computed to be -0.337 and 80.94 , respectively. The InterProScan analysis revealed that the protein sequence belongs to the L-AI family (IPR003762) and has FucI/AraA N-terminal and middle domains (SSF53743) as well as L-AI C-terminal domain (IPR024664). The deduced amino acid sequence of the *araA* derived from *B. amyloliquefaciens* was scanned for conserved residues by the CDD, and the results revealed that the protein contains a conserved domain of L-AI superfamily (CDD accession: cl29844) and L-AI domains (CDD accession: PRK02929, cd03557, and COG2160). The structural modeling of L-AI derived from *B. amyloliquefaciens* CAAI predicted the presence of four Mn^{2+} -binding residues, particularly E307, E332, H349, and H447 (Figure 5). In silico characterization using the Dipro tool indicated the existence of four cysteine residues and predicted the presence of two disulfide bonds (the probable cysteine pairs were C37/C74 and C354/C450).

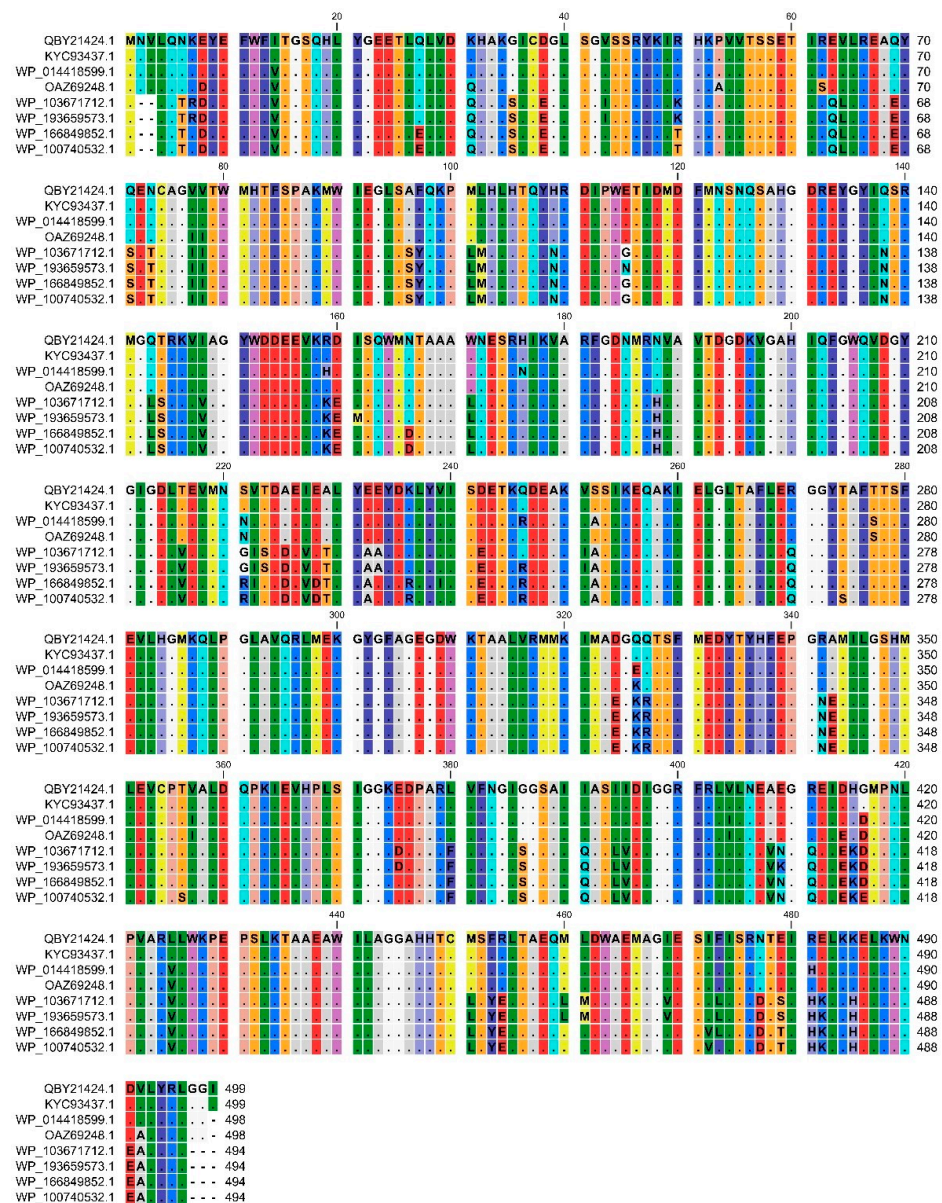


Figure 4. Multiple sequence alignments of the putative L-AI derived from *B. amyloliquefaciens* CAAI with that of other bacterial species. The sequence alignment was conducted using CLC Main Workbench program (version 6.5). The identical residues are indicated as dots.

Table 1. Physicochemical parameters of the putative L-AI derived from *B. amyloliquefaciens* CAAI computed using ExPASy's ProtParam tool.

Parameter	BAAI
Number of amino acids	499
Molecular weight (kDa)	56.41
pI	5.45
Total number of negatively charged residues	70
Total number of positively charged residues	52
GRAVY	−0.337
Instability index	35.77
Aliphatic index	80.94

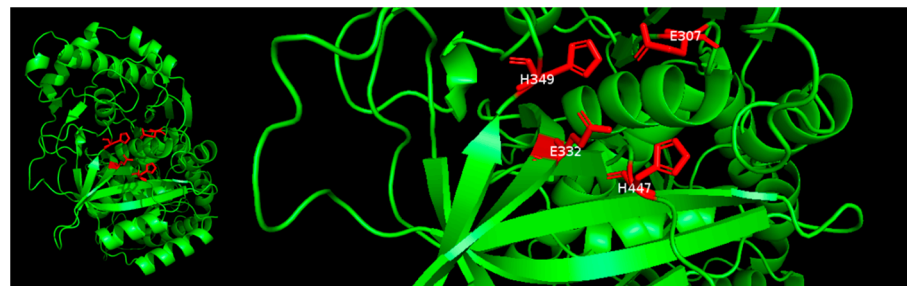


Figure 5. The predicted structure of L-AI derived from *B. amyloliquefaciens* CAAI indicating the metal-binding residues.

3.3. Expression and Characterization of L-AI

The investigated L-AI gene was successfully expressed in *E. coli* as a soluble protein upon induction with IPTG. The His₆-tagged recombinant L-AI gene derived from *B. amyloliquefaciens* (BAAI) was purified from the cell lysate to apparent homogeneity via Ni-NTA affinity chromatography, yielding a single distinct band with an apparent molecular mass of approximately 59 kDa on SDS-PAGE (Figure 6).

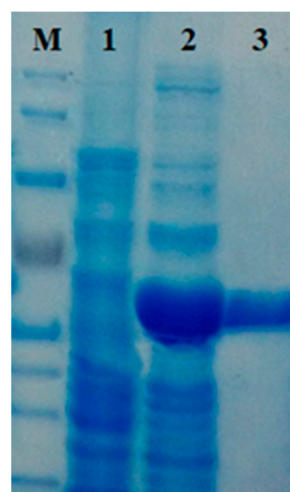


Figure 6. SDS-PAGE showing expression and purification of the His-tagged BAAI derived from *B. amyloliquefaciens* CAAI. Lane 1, molecular weight marker; lane 2, total soluble proteins of uninduced recombinant *E. coli* BL21; lane 3, total soluble proteins of IPTG-induced recombinant *E. coli* BL21; lane 4, Ni-NTA-purified His-tagged L-AI (≈59 kDa).

The results revealed that the recombinant His-tagged enzyme was expressed in an active form with a specific activity of 28 U/mg protein. The influence of temperature on the activity of the recombinant BAAI was assayed in the range of 20 to 70 °C (Figure 7A). The optimum activity was observed at 45 °C. However, BAAI exhibited feasible activity at the investigated temperature range. It showed 39.1% of its maximum activity at 20 °C and more than 52% of the maximum activity at 70 °C. The optimum pH value for BAAI was found to be 7.5 (Figure 7B). The impact of various metal ions on the activity of the recombinant BAAI was investigated. The results showed that the metal-free BAAI retained about 94 and 96% of its initial activity when treated with EDTA and 1,10-phenanthroline, respectively. Regarding thermal stability, BAAI retained about 84 and 60% of its initial activity after pre-treatment for 120 min at 60 and 70 °C, respectively. On the other hand, the metal-free BAAI retained only 38% of its initial activity after pre-treatment for 120 min at 60 °C and completely inhibited after pre-treatment for the same time at 70 °C (Figure 8). Moreover, the activity of the purified metal-free enzyme was estimated in the presence of various divalent metal ions (Table 2). The enzyme was completely inhibited by Pb^{2+} , Cr^{2+} , Ba^{2+} , and Hg^{2+} . On the other hand, BAAI activity was enhanced by 60 and 65% in the presence of Mg^{2+} and Mn^{2+} , respectively. The K_m values of BAAI for D-galactose and L-arabinose were 251.6 mM and 92.8 mM, respectively. The k_{cat} values of the recombinant enzyme were 589.5 and 4350 min^{-1} with D-galactose and L-arabinose, respectively. The catalytic efficiency (k_{cat}/K_m) values for D-galactose and L-arabinose were found to be 2.34 and 46.85 $\text{mM}^{-1} \text{min}^{-1}$, respectively.

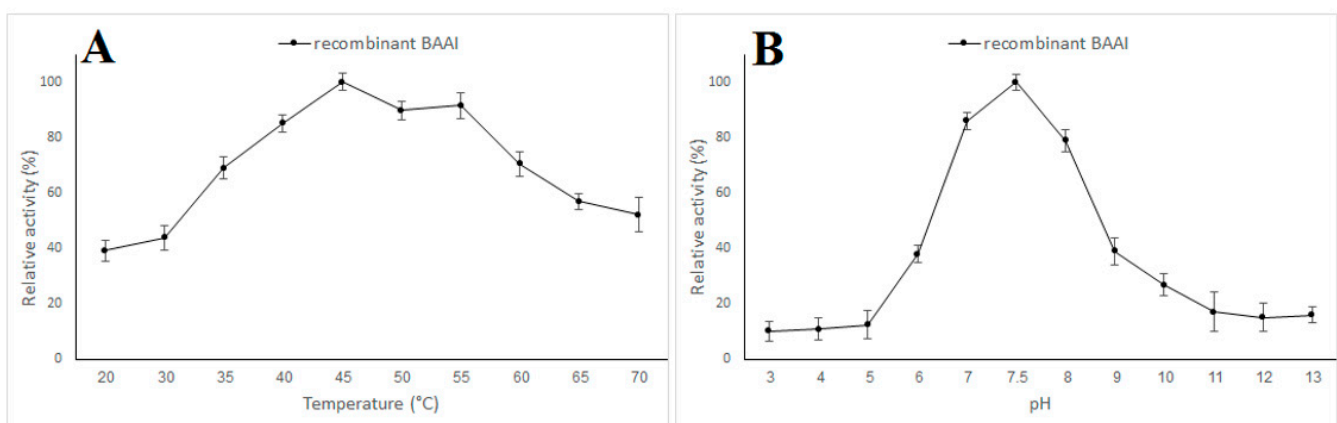


Figure 7. Temperature (A) and pH (B) profiles of the recombinant BAAI derived from *B. amyloliquefaciens* CAAI.

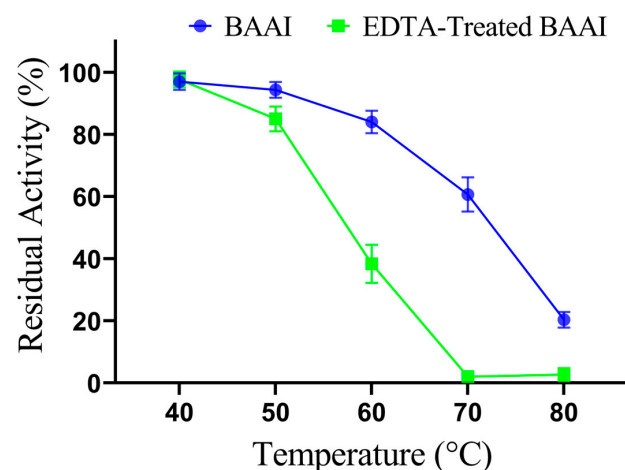


Figure 8. Thermal stability of BAAI and EDTA-Treated BAAI after pre-incubation at various temperatures for 120 min.

Table 2. Influence of various metal ions on the activity of BAAI derived from *B. amyloliquefaciens* CAAI.

Treatment	Relative Activity (%)
Control *	100 ^d
EDTA-Treated L-AI **	94 ^e ± 2
1,10-phenanthroline-Treated L-AI ***	96 ^e ± 1.2
Pb ²⁺	0 ⁱ
Cr ²⁺	0 ⁱ
Cu ²⁺	125 ^c ± 5
Zn ²⁺	46 ^g ± 2
Ba ²⁺	0 ⁱ
Sn ²⁺	120 ^b ± 3
Mg ²⁺	160 ^a ± 5
Ca ²⁺	33 ^h ± 5
Hg ²⁺	0 ⁱ
Mn ²⁺	165 ^a ± 3
Co ²⁺	74 ^f ± 4

The same letter in each column indicates no significant difference according to Duncan's multiple range test ($p < 0.05$). Symbol: ± represents standard deviation. * Enzyme without EDTA treatment and the enzyme assay performed without any metal ion. ** Enzyme treated with EDTA, and the enzyme assay performed without any metal ion. *** Enzyme treated with 1,10-phenanthroline, and the enzyme assay performed without any metal ion.

3.4. Bioconversion of D-Galactose into D-Tagatose by BAAI

The bioconversion catalytic potential of BAAI derived from *B. amyloliquefaciens* strain CAAI was assessed by incubating the purified recombinant enzyme with D-galactose solution for 24 h under the optimum pH (7.5) and temperature (45 °C). The results revealed the production of 47.2 g/L D-tagatose from D-galactose (100 g/L) with 47.2% bioconversion efficiency in a metallic-ions-free reaction system (Figure 9).

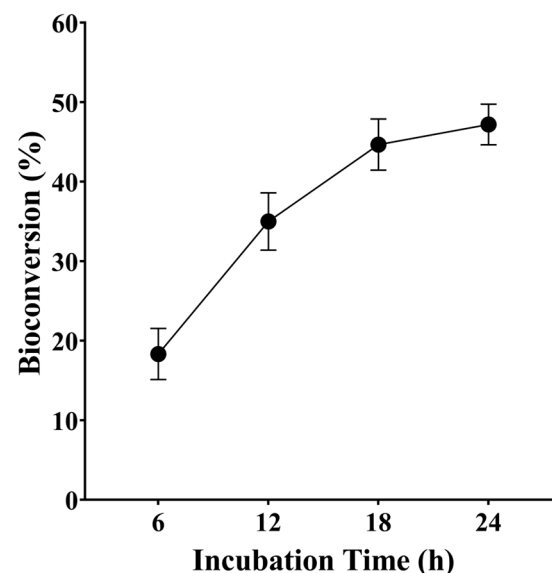


Figure 9. Bioconversion efficacy of D-galactose into D-tagatose by L-AI derived from *B. amyloliquefaciens* strain CAAI under the optimum conditions.

4. Discussion

In this study, fourteen L-AI-producing endophytes were isolated from cantaloupe fruits. Though L-AI-producing bacteria had been isolated from various sources, rare data reporting the endophytic producers are available. The two most active strains regarding L-AI production were identified by 16S rRNA gene sequence analysis as *B. amyloliquefaciens* strain CAAI. Notably and to the best of our knowledge, this study is the first report

describing L-AI production by *B. amyloliquefaciens*; however, enzyme production by other species belonging to the genus *Bacillus* has been documented [41,53,54].

The putative L-AI gene fragment (*araA*) from the *B. amyloliquefaciens* strain CAAI was amplified via PCR, yielding a 1500 bp amplicon. Sequencing analysis confirmed the in-frame cloning of the *araA* gene from the *B. amyloliquefaciens* strain CAAI and revealed an ORF of 1500 bp, which codes for a protein of 499 amino acids. The nucleotide number of the ORF of the *araA* gene from the *B. amyloliquefaciens* strain CAAI is more than that of *Bacillus coagulans* NL01, which contains 1422 bp [55]. Nevertheless, larger ORFs of the *araA* gene from various bacteria have been reported. The ORF of *araA* from *Bifidobacterium adolescentis* encoding L-AI was found to be 1515 bp long and encoding a polypeptide with 504 amino acids [56]. Also, the ORF of the *araA* gene of *Mycobacterium smegmatis* SMDU consisted of 1503 bp encoding 501 amino acid residues [57]. In this study, BLASTp analysis of the deduced amino acid sequence of the investigated gene clustered it within the bacterial L-AI. In silico characterization revealed the component belonging to the L-AI superfamily containing L-AI conserved domains. Furthermore, in silico characterization sheds light on the structure and stability of the investigated protein. The predicted instability index of the enzyme molecule is less than 40, classifying it as a stable protein. In addition, the predicted aliphatic index of BAAI was more than 80, suggesting its thermal stability [58]. BAAI contains more negatively charged residues than positively charged ones. Thus, the enzyme is negatively charged; hence, it could bind water tightly and maintain solvation and solubility, promoting the enzyme function in low water activity conditions [59]. Furthermore, it has been thought that the negatively charged amino acid residues tend to bind with the metal ions leading to an increase in the structural stability of the protein [60,61].

In this study, *araA* gene fragment from the *B. amyloliquefaciens* strain CAAI was effectively expressed in *E. coli*. The recombinant enzyme fraction was purified to homogeneity via affinity chromatography yielding a single distinct band with an apparent molecular mass of approximately 59 kDa on SDS-PAGE. The obtained molecular mass is slightly larger than the actual predicted molecular mass due to the presence of the histidine tag at the N-terminal end of the expressed protein. In relatively good agreement, the molecular weight of a recently reported L-AI derived from *Lactobacillus brevis* was found to be 60.1 kDa via SDS-PAGE analysis [62]. In a similar study, the *araA* gene (1.5 kb) encoding L-AI was cloned, expressed in *E. coli* BL21(DE3) as an N-terminal 6- his-tagged protein, and the purified enzyme showed an apparent molecular mass of 56 kDa by SDS-PAGE, after removing the His-tag residues [63]. Generally, the molecular weight of most documented L-AIs from various bacterial strains ranged from 53 to 66 kDa [64,65].

It has been believed that enzymatic activity and bioconversion efficacy are directly influenced by the reaction conditions such as temperature and pH [66–68]. The purified BAAI was functional and exhibited maximum activity at 45 °C. This operating temperature is slightly greater than that of L-AI derived from *Pseudoalteromonas haloplanktis* that exhibited maximum activity at 40 °C [45] but lower than that of *Bifidobacterium longum* NRRL B-41409 [69]. Nevertheless, various L-AI enzymes showing much higher optimum temperatures (up to 95 °C), such as those from *Thermanaeromonas toyohensis* and *Anoxybacillus flavithermus*, have been reported [39,65]. The pH activity profile of the recombinant BAAI indicated their optimal pH at 7.5. This finding is in context with most reported L-AIs, having maximum activity at pH between 7 and 8 [45,70,71]. More so, the maximum activity of some L-AI enzymes was observed at alkaline conditions showing optimum pH values of 9.0 or above [39,62,72]. On the other hand, few L-AI enzymes were active at an acidic pH range [44,73–75]. Regarding the impact of metal ions on BAAI activities, the results showed that the metal-free BAAI retained about 94% of its original activity. In a similar way, the enzyme was quite active upon treatment with 1,10-phenanthroline as a chelating agent, confirming its metal-dependency. It is worth mentioning that the enzymatic activity of most previously reported L-AI enzymes was inhibited upon treatment with EDTA. The remarkable catalytic activity of BAAI derived from *B. amyloliquefaciens* strain CAAI in the presence of EDTA proposed its ion-independent nature as an extraordinary merit compared

with the most investigated L-AIs in the literature. The activity of BAAI upon treatment with EDTA may be due to the existence of two sulphide bonds that could maintain the structural integrity of the protein after the removal of Mn^{2+} by the chelating agents. Being fairly active in the absence of metal ions, BAAI derived from *B. amyloliquefaciens* strain CAAI could be a promising candidate for applications in the production of D-tagatose without the need for any health-threatening metal ions. On the other hand, the activity of the L-AI from *Geobacillus stearothermophilus* DSM 22 is completely metal-dependent [76]. The crystal structure of L-AI derived from *E. coli* provided an unswerving insight into the crucial role of certain metal ions in the catalytic activity of these enzymes being located in the active sites of the enzyme [77]. Moreover, the role of certain metal ions in the catalytic activity of L-AIs derived from *Geobacillus kaustophilus* has been elucidated [63]. Our results indicated that Mn^{2+} was unnecessary for the enzymatic activity of BAAI but has a vital role in enhancing the thermal stability of the BAAI. These findings agree with previous studies that described the role of Mn^{2+} in keeping the structural integrity of various L-AIs at elevated temperatures. As the optimum temperature of BAAI derived from *B. amyloliquefaciens* strain CAAI was 45 °C, it can operate to convert D-galactose to D-tagatose without the need for Mn^{2+} , providing two advantages. The first is working at relatively lower temperatures, which reduces energy consumption. The second advantage is the lack of metal ions for the bioconversion process, which increases its safety. The high thermal stability of an enzyme is a vital property for successful industrial applications. Regarding D-tagatose production, thermostable L-AIs have advantages such as reduced formation of unwanted, faster reaction rates equilibrium shifts toward D-tagatose [30]. It is widely accepted that the elevated operating temperatures reduce the viscosity of reaction mixtures and increase the solubility of substrates, leading to improved reaction rates. The present study indicated the feasible thermal stability of BAAI that retained about 84 and 60% of its initial activity after pre-treatment for 120 min at 60 and 70 °C, respectively. This thermostability is comparable to that of some thermostable L-AIs derived from mesophilic strains such as *Lactobacillus plantarum* NC8 L-AI, which is perfectly stable after a 2 h incubation at 70 °C [78]. Generally, enzymes derived from thermophilic and hyperthermophilic microorganisms have excellent thermal stability. It has been reported that L-AI derived from *Thermotoga maritima* can retain more than 50% of its initial activity after incubation for 120 min at 90 °C [79]. However, the thermostability of enzymes derived from mesophilic microorganisms could be improved via immobilization [80]. The kinetic parameters of BAAI derived from *B. amyloliquefaciens* strain CAAI were compared with those of various bacterial L-AIs (Table 3). The K_m value of BAAI derived from *B. amyloliquefaciens* strain CAAI was 251.6 mM. This result is comparable to that of L-AIs derived from *Enterococcus faecium* DBFIQ E36, *Bacillus subtilis*, and *Thermotoga neapolitana* [81–83]. The K_m value of the enzymes varies by different sources depending on their sequences and structures, which reflect the specificity and activity of the enzymes to their substrates. The lower the k_m value, the higher specificity and activity. The K_m value of the L-AI derived from *Geobacillus thermodenitrificans* was 408 mM [84]. On the other hand, various L-AIs derived from various microbial sources exhibited lower K_m values. In a recent study, the K_m value of a highly D-galactose-specific L-AI from *Bifidobacterium adolescentis* was 22.4 mM [56]. Also, L-AIs derived from *Clostridium hylemonae* 15,053 had a K_m value of 7.7 mM [85]. Notably, BAAI derived from *B. amyloliquefaciens* strain CAAI exhibited higher affinity L-arabinose than that toward D-galactose. These findings are in line with the most described bacterial L-AIs. On the contrary, L-AIs derived from *Anoxybacillus flavithermus* and *Bifidobacterium adolescentis* had a higher affinity toward D-galactose than that toward L-arabinose. As summarized in Table 3, our results indicated that the catalytic efficiency (k_{cat}/K_m) of BAAI derived from *B. amyloliquefaciens* strain CAAI with D-galactose as a substrate is superior to that of L-AIs derived from *Bacillus coagulans*, *Enterococcus faecium*, *Geobacillus thermodenitrificans*; however, it is lower than that of *Geobacillus stearothermophilus*, *Lactobacillus reuteri*, *A. flavithermus* and *B. adolescentis*. In the present study, the recombinant L-AI enzyme (BAAI) derived from *B. amyloliquefaciens* strain CAAI showed a distinguished isomerization activity of

D-galactose to D-tagatose with bioconversion efficiency of 47.2%. This productivity is equivalent to that of L-AI derived from *Lactobacillus brevis* [62]. The productivity of the BAAI described in the present paper is much higher than that described by L-AI derived from *Bacillus coagulans* NL01, exhibiting a conversion rate of 32% after 32 h [55]. However, higher conversion efficiencies have been documented. The bioconversion efficacy of L-AI derived from *B. adolescentis* was 56.7% at 55 °C and pH 6.5 after 10 h [85]. The recombinant L-AI derived from *B. subtilis* DSM-92 isomerized D-galactose to D-tagatose, with ~59% conversion after 24 h at 42 °C and pH 7.5 [35]. It has been suggested that the maximization of enzyme productivity requires the optimization of various key reaction parameters such as pH, temperature, and concentrations as well as other parameters, including the selection of enzyme sources and additives, mode of operation, and the reactor design [86].

Table 3. Kinetic parameters of various bacterial L-Ais.

Organism	L-Arabinose			D-Galactose			Reference
	K_m (mM)	K_{cat} (min^{-1})	K_{cat}/K_m ($\text{mM}^{-1} \text{min}^{-1}$)	K_m (mM)	K_{cat} (min^{-1})	K_{cat}/K_m ($\text{mM}^{-1} \text{min}^{-1}$)	
<i>B. amyloliquefaciens</i>	92.84	4350	46.85	251.6	589.5	2.34	This study
<i>Geobacillus stearothermophilus</i>	77.0	4515	58.0	279.0	3185	11.4	[82]
<i>Lactobacillus reuteri</i>	633.0	57,540	90.0	647.0	3540	5.4	[87]
<i>Anoxybacillus flavithermus</i>	78.5	52.8	0.67	25.1	129.9	5.1	[39]
<i>Geobacillus thermodenitrificans</i>	142.0	NR	48	408.0	NR	0.5	[84]
<i>Bacillus licheniformis</i>	369.0	12,450	34.0	NR	NR	NR	[88]
<i>Lactobacillus sakai</i>	32.0	3516	109.2	NR	NR	NR	[32]
<i>Bifidobacterium adolescentis</i>	40.2	NR	8.6	22.4	NR	9.3	[56]
<i>Enterococcus faecium</i>	NR	NR	NR	225.0	151	0.68	[37]
<i>Bacillus coagulans</i>	269.8	NR	8.7	355.1	NR	1.0	[55]
<i>Bacillus velezensis</i>	194.6	2067.3	10.58	NR	NR	NR	[89]

5. Conclusions

In this work, we cloned, expressed, and characterized L-AI from a newly isolated endophytic *B. amyloliquefaciens* strain CAAI. The purified enzyme with a molecular weight of 59 kDa exhibited a specific activity of 28 U/mg protein and maximal activity at pH 7.5 and 45 °C. Remarkably, the enzyme is quite active without metallic ions and produced D-tagatose from D-galactose with a bioconversion efficiency of 47.2% in a metallic-ions-free reaction system. Though the enzyme was quite active in the absence of metal ions, Mn^{2+} boosted its thermal stability, suggesting its crucial role in maintaining the structural integrity of the enzyme at high temperatures. This investigation highlighted the biochemical properties of the metallic-ions-independent L-AI from *B. amyloliquefaciens* as an attractive choice to implement in the safe production of food-grade low-calorie sweetener, D-tagatose.

Author Contributions: Conceptualization, M.G.F.; Methodology, H.M.S. and M.G.F.; Software, M.G.F.; Validation, M.G.F.; Investigation, H.M.S. and M.G.F.; Resources, M.N.A.E.-G., S.A.H., M.M.A., K.I.G. and M.G.F.; Data curation, M.G.F.; Writing—original draft, H.M.S., M.N.A.E.-G. and M.G.F.; Writing—review & editing, M.G.F.; Visualization, M.G.F.; Supervision, Z.K. and M.G.F.; Funding acquisition, S.A.H., M.M.A. and K.I.G. All authors have read and agreed to the published version of the manuscript.

Funding: This research received no external funding.

Institutional Review Board Statement: Not applicable.

Informed Consent Statement: Not applicable.

Data Availability Statement: The essential data supporting the reported results are contained in this study. All other data are available upon request from the corresponding authors.

Acknowledgments: The authors are thankful to the Deanship of Scientific Research at University of Bisha for supporting this work through the Fast-Track Research Support Program.

Conflicts of Interest: The authors declare no conflict of interest.

References

1. Levin, G.V. Tagatose, the New GRAS Sweetener and Health Product. *J. Med. Food* **2004**, *5*, 23–36. [[CrossRef](#)] [[PubMed](#)]
2. Van Laar, A.D.E.; Grootaert, C.; Van Camp, J. Rare Mono- and Disaccharides as Healthy Alternative for Traditional Sugars and Sweeteners? *Crit. Rev. Food Sci. Nutr.* **2020**, *61*, 713–741. [[CrossRef](#)] [[PubMed](#)]
3. Ravikumar, Y.; Ponpandian, L.N.; Zhang, G.; Yun, J.; Qi, X. Harnessing L-Arabinose Isomerase for Biological Production of d-Tagatose: Recent Advances and Its Applications. *Trends Food Sci. Technol.* **2021**, *107*, 16–30. [[CrossRef](#)]
4. Han, P.; Wang, X.; Li, Y.; Wu, H.; Shi, T.; Shi, J. Synthesis of a Healthy Sweetener D-Tagatose from Starch Catalyzed by Semiartificial Cell Factories. *J. Agric. Food Chem.* **2023**, *71*, 3813–3820. [[CrossRef](#)]
5. Donner, T.W.; Magder, L.S.; Zarbalian, K. Dietary Supplementation with D-Tagatose in Subjects with Type 2 Diabetes Leads to Weight Loss and Raises High-Density Lipoprotein Cholesterol. *Nutr. Res.* **2010**, *30*, 801–806. [[CrossRef](#)]
6. Lo, M.C.; Lansang, M.C. Recent and Emerging Therapeutic Medications in Type 2 Diabetes Mellitus: Incretin-Based, Pramlintide, Colesevelam, SGLT2 Inhibitors, Tagatose, Succinobucol. *Am. J. Ther.* **2013**, *20*, 638–653. [[CrossRef](#)]
7. Ahmed, A.; Khan, T.A.; Ramdath, D.D.; Kendall, C.W.C.; Sievenpiper, J.L.; Ahmed, A.; Khan, T.A.; Kendall, C.W.C.; Sievenpiper, J.L. Rare Sugars and Their Health Effects in Humans: A Systematic Review and Narrative Synthesis of the Evidence from Human Trials. *Nutr. Rev.* **2022**, *80*, 255–270. [[CrossRef](#)]
8. Kwak, J.H.; Kim, M.S.; Lee, J.H.; Yang, Y.J.; Lee, K.H.; Kim, O.Y.; Lee, J.H. Beneficial Effect of Tagatose Consumption on Postprandial Hyperglycemia in Koreans: A Double-Blind Crossover Designed Study. *Food Funct.* **2013**, *4*, 1223–1228. [[CrossRef](#)]
9. Police, S.B.; Harris, J.C.; Lodder, R.A.; Cassis, L.A. Effect of Diets Containing Sucrose vs. D-Tagatose in Hypercholesterolemic Mice. *Obesity* **2009**, *17*, 269–275. [[CrossRef](#)]
10. Hasibul, K.; Nakayama-Imaohji, H.; Hashimoto, M.; Yamasaki, H.; Ogawa, T.; Waki, J.; Tada, A.; Yoneda, S.; Tokuda, M.; Miyake, M.; et al. D-Tagatose Inhibits the Growth and Biofilm Formation of *Streptococcus Mutans*. *Mol. Med. Rep.* **2018**, *17*, 843–851. [[CrossRef](#)]
11. Ensor, M.; Banfield, A.B.; Smith, R.R.; Williams, J.; Lodder, R.A. Safety and Efficacy of D-Tagatose in Glycemic Control in Subjects with Type 2 Diabetes. *J. Endocrinol. Diabetes Obes.* **2014**, *3*, 1065. [[PubMed](#)]
12. Guerrero-Wyss, M.; Durán Agüero, S.; Angarita Dávila, L. D-Tagatose Is a Promising Sweetener to Control Glycaemia: A New Functional Food. *Biomed. Res. Int.* **2018**, *2018*, 8718053. [[CrossRef](#)] [[PubMed](#)]
13. Mooradian, A.D.; Haas, M.J.; Onstead-Haas, L.; Tani, Y.; Iida, T.; Tokuda, M. Naturally Occurring Rare Sugars Are Free Radical Scavengers and Can Ameliorate Endoplasmic Reticulum Stress. *Int. J. Vitam. Nutr. Res.* **2019**, *90*, 210–220. [[CrossRef](#)]
14. Valeri, F.; Boess, F.; Wolf, A.; Goldlin, C.; Boelsterli, U.A. Fructose and Tagatose Protect against Oxidative Cell Injury by Iron Chelation. *Free Radic. Biol. Med.* **1997**, *22*, 257–268. [[CrossRef](#)]
15. Paterna, J.C.; Boess, F.; Staubli, A.; Boelsterli, U.A. Antioxidant and Cytoprotective Properties of D-Tagatose in Cultured Murine Hepatocytes. *Toxicol. Appl. Pharmacol.* **1998**, *148*, 117–125. [[CrossRef](#)]
16. Rojo-Poveda, O.; Barbosa-Pereira, L.; Orden, D.; Stévigny, C.; Zeppa, G.; Bertolino, M. Physical Properties and Consumer Evaluation of Cocoa Bean Shell-Functionalized Biscuits Adapted for Diabetic Consumers by the Replacement of Sucrose with Tagatose. *Foods* **2020**, *9*, 814. [[CrossRef](#)]
17. Mayumi, S.; Kuboniwa, M.; Sakanaka, A.; Hashino, E.; Ishikawa, A.; Ijima, Y.; Amano, A. Potential of Prebiotic D-Tagatose for Prevention of Oral Disease. *Front. Cell Infect. Microbiol.* **2021**, *11*, 767944. [[CrossRef](#)]
18. Huang, J.; Wang, B.; Tao, S.; Hu, Y.; Wang, N.; Zhang, Q.; Wang, C.; Chen, C.; Gao, B.; Cheng, X.; et al. D-Tagatose Protects against Oleic Acid-Induced Acute Respiratory Distress Syndrome in Rats by Activating PTEN/PI3K/AKT Pathway. *Front. Immunol.* **2022**, *13*, 928312. [[CrossRef](#)]
19. Roy, S.; Chikkerur, J.; Roy, S.C.; Dhali, A.; Kolte, A.P.; Sridhar, M.; Samanta, A.K. Tagatose as a Potential Nutraceutical: Production, Properties, Biological Roles, and Applications. *J. Food Sci.* **2018**, *83*, 2699–2709. [[CrossRef](#)]
20. Chahed, A.; Nesler, A.; Aziz, A.; Barka, E.A.; Pertot, I.; Perazzolli, M. A Review of Knowledge on the Mechanisms of Action of the Rare Sugar D-Tagatose against Phytopathogenic Oomycetes. *Plant Pathol.* **2021**, *70*, 1979–1986. [[CrossRef](#)]
21. Mijailovic, N.; Richet, N.; Villaume, S.; Nesler, A.; Perazzolli, M.; Barka, E.A.; Aziz, A. D-Tagatose-Based Product Triggers Sweet Immunity and Resistance of Grapevine to Downy Mildew, but Not to Gray Mold Disease. *Plants* **2022**, *11*, 296. [[CrossRef](#)] [[PubMed](#)]
22. Chahed, A.; Nesler, A.; Esmaeel, Q.; Barka, E.A.; Perazzolli, M. The Amount of the Rare Sugar Tagatose on Tomato Leaves Decreases after Spray Application under Greenhouse Conditions. *Plants* **2022**, *11*, 2781. [[CrossRef](#)]
23. Corneo, P.E.; Jermini, M.; Nadalini, S.; Giovannini, O.; Nesler, A.; Perazzolli, M.; Pertot, I. Foliar and Root Applications of the Rare Sugar Tagatose Control Powdery Mildew in Soilless Grown Cucumbers. *Crop Prot.* **2021**, *149*, 105753. [[CrossRef](#)]

24. Armstrong, L.M.; Luecke, K.J.; Bell, L.N. Consumer Evaluation of Bakery Product Flavour as Affected by Incorporating the Prebiotic Tagatose. *Int. J. Food Sci. Technol.* **2009**, *44*, 815–819. [[CrossRef](#)]
25. Mijailovic, N.; Nesler, A.; Perazzolli, M.; Ait Barka, E.; Aziz, A. Rare Sugars: Recent Advances and Their Potential Role in Sustainable Crop Protection. *Molecules* **2021**, *26*, 1720. [[CrossRef](#)]
26. Farahat, M.G.; Shehata, H.M.; Kamel, Z. Codon Optimization and Co-Expression of Thermostable β -Galactosidase and L-Arabinose Isomerase in *Lactococcus Lactis* for Single-Step Production of Food-Grade D-Tagatose. *Biochem. Cell Arch.* **2020**, *20*, 2545–2552.
27. Guo, Q.; An, Y.; Yun, J.; Yang, M.; Magocha, T.A.; Zhu, J.; Xue, Y.; Qi, Y.; Hossain, Z.; Sun, W.; et al. Enhanced D-Tagatose Production by Spore Surface-Displayed L-Arabinose Isomerase from Isolated *Lactobacillus Brevis* PC16 and Biotransformation. *Bioresour. Technol.* **2018**, *247*, 940–946. [[CrossRef](#)]
28. Xu, Z.; Li, S.; Feng, X.; Liang, J.; Xu, H. L-Arabinose Isomerase and Its Use for Biotechnological Production of Rare Sugars. *Appl. Microbiol. Biotechnol.* **2014**, *98*, 8869–8878. [[CrossRef](#)] [[PubMed](#)]
29. Han, Z.; Li, N.; Xu, H.; Xu, Z. Improved Thermostability and Robustness of L-Arabinose Isomerase by C-Terminal Elongation and Its Application in Rare Sugar Production. *Biochem. Biophys. Res. Commun.* **2022**, *637*, 224–231. [[CrossRef](#)]
30. Xu, W.; Zhang, W.; Zhang, T.; Jiang, B.; Mu, W. L-Arabinose Isomerases: Characteristics, Modification, and Application. *Trends Food Sci. Technol.* **2018**, *78*, 25–33. [[CrossRef](#)]
31. Li, J.; Wu, J.; Chen, S.; Xia, W. Rational Design of L-Arabinose Isomerase from *Lactobacillus Fermentum* and Its Application in D-Tagatose Production. *Chin. J. Biotechnol.* **2023**, *39*, 1107–1118. [[CrossRef](#)]
32. Singh, A.; Rai, S.K.; Yadav, S.K. Metal-Based Micro-Composite of L-Arabinose Isomerase and L-Ribose Isomerase for the Sustainable Synthesis of L-Ribose and D-Talose. *Colloids Surf. B Biointerfaces* **2022**, *217*, 112637. [[CrossRef](#)] [[PubMed](#)]
33. Seo, C.; Kim, M.-J.; Kim, S.J.; Park, Y.-S.; Shin, K.-C.; Seo, M.-J.; Kim, S.J.; Kim, Y.-S.; Park, C.-S. Characterization of L-Arabinose Isomerase from *Klebsiella Pneumoniae* and Its Application in the Production of d-Tagatose from d-Galactose. *Appl. Sci.* **2022**, *12*, 4696. [[CrossRef](#)]
34. Zhang, S.; Xu, Z.; Ma, M.; Zhao, G.; Chang, R.; Si, H.; Dai, M. A Novel *Lactococcus Lactis* L-Arabinose Isomerase for d-Tagatose Production from Lactose. *Food Biosci.* **2022**, *48*, 101765. [[CrossRef](#)]
35. Baptista, S.L.; Román, A.; Oliveira, C.; Ferreira, S.; Rocha, C.M.R.; Domingues, L. Galactose to Tagatose Isomerization by the L-Arabinose Isomerase from *Bacillus Subtilis*: A Biorefinery Approach for *Gelidium Sesquipedale* Valorisation. *LWT* **2021**, *151*, 112199. [[CrossRef](#)]
36. Jayaraman, A.B.; Kandasamy, T.; Venkataraman, D.; Meenakshisundaram, S. Rational Design of *Shewanella* sp. L-Arabinose Isomerase for d-Galactose Isomerase Activity under Mesophilic Conditions. *Enzym. Microb. Technol.* **2021**, *147*, 109796. [[CrossRef](#)]
37. de Souza, T.C.; Oliveira, R.C.; Bezerra, S.G.S.; Manzo, R.M.; Mammarella, E.J.; Hissa, D.C.; Gonçalves, L.R.B. Alternative Heterologous Expression of L-Arabinose Isomerase from *Enterococcus faecium* DBFIQ E36 by Residual Whey Lactose Induction. *Mol. Biotechnol.* **2021**, *63*, 289–304. [[CrossRef](#)]
38. Fan, C.; Liu, K.; Zhang, T.; Zhou, L.; Xue, D.; Jiang, B.; Mu, W. Biochemical Characterization of a Thermostable L-Arabinose Isomerase from a Thermoacidophilic Bacterium, *Alicyclobacillus Hesperidum* URH17-3-68. *J. Mol. Catal. B Enzym.* **2014**, *102*, 120–126. [[CrossRef](#)]
39. Li, Y.; Zhu, Y.; Liu, A.; Sun, Y. Identification and Characterization of a Novel L-Arabinose Isomerase from *Anoxybacillus Flavithermus* Useful in d-Tagatose Production. *Extremophiles* **2011**, *15*, 441–450. [[CrossRef](#)]
40. Wanarska, M.; Kur, J. A Method for the Production of D-Tagatose Using a Recombinant *Pichia Pastoris* Strain Secreting β -D-Galactosidase from *Arthrobacter chlorophenolicus* and a Recombinant L-Arabinose Isomerase from *Arthrobacter* sp. 22c. *Microb. Cell Fact.* **2012**, *11*, 113. [[CrossRef](#)]
41. Seo, M.-J. Characterization of an L-Arabinose Isomerase from *Bacillus Thermoglucosidasius* for D-Tagatose Production. *Biosci. Biotechnol. Biochem.* **2013**, *77*, 385–388. [[CrossRef](#)] [[PubMed](#)]
42. Laksmi, F.A.; Arai, S.; Tsurumaru, H.; Nakamura, Y.; Saksono, B.; Tokunaga, M.; Ishibashi, M. Improved Substrate Specificity for D-Galactose of L-Arabinose Isomerase for Industrial Application. *Biochim. Biophys. Acta Proteins Proteom.* **2018**, *1866*, 1084–1091. [[CrossRef](#)] [[PubMed](#)]
43. Zhang, G.; Zaved, H.M.; Yun, J.; Yuan, J.; Zhang, Y.; Wang, Y.; Qi, X. Two-Stage Biosynthesis of D-Tagatose from Milk Whey Powder by an Engineered *Escherichia Coli* Strain Expressing L-Arabinose Isomerase from *Lactobacillus Plantarum*. *Bioresour. Technol.* **2020**, *305*, 123010. [[CrossRef](#)] [[PubMed](#)]
44. Men, Y.; Zhu, Y.; Zhang, L.; Kang, Z.; Izumori, K.; Sun, Y.; Ma, Y. Enzymatic Conversion of D-Galactose to d-Tagatose: Cloning, Overexpression and Characterization of L-Arabinose Isomerase from *Pediococcus Pentosaceus* PC-5. *Microbiol. Res.* **2014**, *169*, 171–178. [[CrossRef](#)]
45. Xu, W.; Fan, C.; Zhang, T.; Jiang, B.; Mu, W. Cloning, Expression, and Characterization of a Novel L-Arabinose Isomerase from the Psychrotolerant Bacterium *Pseudoalteromonas Haloplanktis*. *Mol. Biotechnol.* **2016**, *58*, 695–706. [[CrossRef](#)]
46. Patel, M.J.; Akhani, R.C.; Patel, A.T.; Dedania, S.R.; Patel, D.H. A Single and Two Step Isomerization Process for D-Tagatose and L-Ribose Bioproduction Using L-Arabinose Isomerase and d-Lyxose Isomerase. *Enzym. Microb. Technol.* **2017**, *97*, 27–33. [[CrossRef](#)]
47. Dische, Z.; Borenfreund, E. A New Spectrophotometric Method for the Detection and Determination of Keto Sugars and Trioses. *J. Biol. Chem.* **1951**, *192*, 583–587. [[CrossRef](#)]

48. El-Ghany, M.N.A.; Hamdi, S.A.; Korany, S.M.; Elbaz, R.M.; Farahat, M.G. Biosynthesis of Novel Tellurium Nanorods by *Gayadomonas* sp. TNPM15 Isolated from Mangrove Sediments and Assessment of Their Impact on Spore Germination and Ultrastructure of Phytopathogenic Fungi. *Microorganisms* **2023**, *11*, 558. [[CrossRef](#)]
49. Quevillon, E.; Silventoinen, V.; Pillai, S.; Harte, N.; Mulder, N.; Apweiler, R.; Lopez, R. InterProScan: Protein Domains Identifier. *Nucleic Acids Res.* **2005**, *33*, W116–W120. [[CrossRef](#)]
50. Gasteiger, E.; Hoogland, C.; Gattiker, A.; Duvaud, S.; Wilkins, M.R.; Appel, R.D.; Bairoch, A. Protein Identification and Analysis Tools on the ExPASy Server. In *The Proteomics Protocols Handbook*; Humana Press: Totowa, NJ, USA, 2005; pp. 571–607.
51. Farahat, M.G.; Amr, D.; Galal, A. Molecular Cloning, Structural Modeling and Characterization of a Novel Glutaminase-Free L-Asparaginase from *Cobetia Amphilecti* AMI6. *Int. J. Biol. Macromol.* **2020**, *143*, 685–695. [[CrossRef](#)]
52. Bradford, M.M. A Rapid and Sensitive Method for the Quantitation of Microgram Quantities of Protein Utilizing the Principle of Protein-Dye Binding. *Anal. Biochem.* **1976**, *72*, 248–254. [[CrossRef](#)] [[PubMed](#)]
53. Zhang, Y.W.; Prabhu, P.; Lee, J.K. Immobilization of *Bacillus Licheniformis* L-Arabinose Isomerase for Semi-Continuous l-Ribulose Production. *Biosci. Biotechnol. Biochem.* **2009**, *73*, 2234–2239. [[CrossRef](#)] [[PubMed](#)]
54. Zheng, Z.; Mei, W.; Xia, M.; He, Q.; Ouyang, J. Rational Design of *Bacillus Coagulans* NL01 L-Arabinose Isomerase and Use of Its F279I Variant in D-Tagatose Production. *J. Agric. Food Chem.* **2017**, *65*, 4715–4721. [[CrossRef](#)] [[PubMed](#)]
55. Mei, W.; Wang, L.; Zang, Y.; Zheng, Z.; Ouyang, J. Characterization of an L-Arabinose Isomerase from *Bacillus Coagulans* NL01 and Its Application for D-Tagatose Production. *BMC Biotechnol.* **2016**, *16*, 55. [[CrossRef](#)]
56. Zhang, G.; An, Y.; Parvez, A.; Zaved, H.M.; Yun, J.; Qi, X. Exploring a Highly D-Galactose Specific L-Arabinose Isomerase from *Bifidobacterium Adolescentis* for D-Tagatose Production. *Front. Bioeng. Biotechnol.* **2020**, *8*, 377. [[CrossRef](#)]
57. Takata, G.; Poonperm, W.; Rao, D.; Souda, A.; Nishizaki, T.; Morimoto, K.; Izumori, K. Cloning, Expression, and Transcription Analysis of L-Arabinose Isomerase Gene from *Mycobacterium Smegmatis* SMDU. *Biosci. Biotechnol. Biochem.* **2007**, *71*, 2876–2885. [[CrossRef](#)]
58. Devi, S.; Sharma, N.; Savitri; Bhalla, T.C. Comparative Analysis of Amino Acid Sequences from Mesophiles and Thermophiles in Respective of Carbon–Nitrogen Hydrolase Family. *3 Biotech* **2013**, *3*, 491–507. [[CrossRef](#)]
59. DasSarma, S.; DasSarma, P. Halophiles and Their Enzymes: Negativity Put to Good Use. *Curr. Opin. Microbiol.* **2015**, *25*, 120–126. [[CrossRef](#)]
60. Selvin, J.; Kennedy, J.; Lejon, D.P.H.; Kiran, G.S.; Dobson, A.D.W. Isolation Identification and Biochemical Characterization of a Novel Halo-Tolerant Lipase from the Metagenome of the Marine Sponge *Haliclona Simulans*. *Microb. Cell Fact.* **2012**, *11*, 72. [[CrossRef](#)]
61. Çolak, A.; Şişik, D.; Sağlam, N.; Güner, S.; Çanakçı, S.; Beldüz, A.O. Characterization of a Thermoalkalophilic Esterase from a Novel Thermophilic Bacterium, *Anoxybacillus Gonensis* G2. *Bioresour. Technol.* **2005**, *96*, 625–631. [[CrossRef](#)]
62. Du, M.; Zhao, D.; Cheng, S.; Sun, D.; Chen, M.; Gao, Z.; Zhang, C. Towards Efficient Enzymatic Conversion of D-Galactose to d-Tagatose: Purification and Characterization of L-Arabinose Isomerase from *Lactobacillus Brevis*. *Bioprocess. Biosyst. Eng.* **2019**, *42*, 107–116. [[CrossRef](#)] [[PubMed](#)]
63. Choi, J.M.; Lee, Y.-J.; Cao, T.-P.; Shin, S.-M.; Park, M.-K.; Lee, H.-S.; di Luccio, E.; Kim, S.-B.; Lee, S.-J.; Lee, S.J.; et al. Structure of the Thermophilic L-Arabinose Isomerase from *Geobacillus Kaustophilus* Reveals Metal-Mediated Intersubunit Interactions for Activity and Thermostability. *Arch. Biochem. Biophys.* **2016**, *596*, 51–62. [[CrossRef](#)] [[PubMed](#)]
64. Prabhu, P.; Kumar Tiwari, M.; Jeya, M.; Gunasekaran, P.; Kim, I.W.; Lee, J.K. Cloning and Characterization of a Novel L-Arabinose Isomerase from *Bacillus Licheniformis*. *Appl. Microbiol. Biotechnol.* **2008**, *81*, 283–290. [[CrossRef](#)] [[PubMed](#)]
65. Iqbal, M.W.; Riaz, T.; Hassanin, H.A.M.; Ni, D.; Mahmood Khan, I.; Rehman, A.; Mahmood, S.; Adnan, M.; Mu, W. Characterization of a Novel D-Arabinose Isomerase from *Thermanaeromonas Toyohensis* and Its Application for the Production of D-Ribulose and L-Fuculose. *Enzym. Microb. Technol.* **2019**, *131*, 109427. [[CrossRef](#)]
66. Saranik, M.M.; Badawy, M.A.; Farahat, M.G. Fabrication of β -Glucosidase–Copper Phosphate Hybrid Nanoflowers for Bioconversion of Geniposide into Gardenia Blue. *Int. J. Nanosci.* **2023**, *22*, 2350040. [[CrossRef](#)]
67. Al-Qaysi, S.A.S.; Al-Haideri, H.; Al-Shimmery, S.M.; Abdulhameed, J.M.; Alajrawy, O.I.; Al-Halbosiy, M.M.; Moussa, T.A.A.; Farahat, M.G. Bioactive Levan-Type Exopolysaccharide Produced by *Pantoea Agglomerans* ZMR7: Characterization and Optimization for Enhanced Production. *J. Microbiol. Biotechnol.* **2021**, *31*, 696–704. [[CrossRef](#)]
68. El-Ghany, M.N.A.; Hamdi, S.A.; Elbaz, R.M.; Aloufi, A.S.; El Sayed, R.R.; Ghonaim, G.M.; Farahat, M.G. Development of a Microbial-Assisted Process for Enhanced Astaxanthin Recovery from Crab Exoskeleton Waste. *Fermentation* **2023**, *9*, 505. [[CrossRef](#)]
69. Salonen, N.; Nyyssölä, A.; Salonen, K.; Turunen, O. *Bifidobacterium Longum* L-Arabinose Isomerase Overexpression in *Lactococcus Lactis*, Purification, and Characterization. *Appl. Biochem. Biotechnol.* **2012**, *168*, 392–405. [[CrossRef](#)]
70. Jung, E.-S.; Kim, H.-J.; Oh, D.-K. Tagatose Production by Immobilized Recombinant *Escherichia Coli* Cells Containing *Geobacillus Stearothermophilus*-L-Arabinose Isomerase Mutant in a Packed-Bed Bioreactor. *Biotechnol. Prog.* **2008**, *21*, 1335–1340. [[CrossRef](#)]
71. Liang, M.; Chen, M.; Liu, X.; Zhai, Y.; Liu, X.W.; Zhang, H.; Xiao, M.; Wang, P. Bioconversion of D-Galactose to D-Tagatose: Continuous Packed Bed Reaction with an Immobilized Thermostable L-Arabinose Isomerase and Efficient Purification by Selective Microbial Degradation. *Appl. Microbiol. Biotechnol.* **2012**, *93*, 1469–1474. [[CrossRef](#)]
72. Lim, B.C.; Kim, H.J.; Oh, D.K. High Production of D-Tagatose by the Addition of Boric Acid. *Biotechnol. Prog.* **2007**, *23*, 824–828. [[CrossRef](#)] [[PubMed](#)]

73. Manzo, R.M.; Antunes, A.S.L.M.; de Sousa Mendes, J.; Hissa, D.C.; Gonçalves, L.R.B.; Mammarella, E.J. Biochemical Characterization of Heat-Tolerant Recombinant L-Arabinose Isomerase from *Enterococcus Faecium* DBFIQ E36 Strain with Feasible Applications in d-Tagatose Production. *Mol. Biotechnol.* **2019**, *61*, 385–399. [[CrossRef](#)] [[PubMed](#)]
74. Lee, S.J.; Lee, D.W.; Choe, E.A.; Hong, Y.H.; Kim, S.B.; Kim, B.C.; Pyun, Y.R. Characterization of a Thermoacidophilic L-Arabinose Isomerase from *Alicyclobacillus Acidocaldarius*: Role of Lys-269 in PH Optimum. *Appl. Environ. Microbiol.* **2005**, *71*, 7888–7896. [[CrossRef](#)] [[PubMed](#)]
75. Wu, H.; Huang, J.; Deng, Y.; Zhang, W.; Mu, W. Production of L-Ribose from L-Arabinose by Co-Expression of L-Arabinose Isomerase and D-Lyxose Isomerase in *Escherichia Coli*. *Enzym. Microb. Technol.* **2020**, *132*, 109443. [[CrossRef](#)] [[PubMed](#)]
76. Lee, D.W.; Choe, E.A.; Kim, S.B.; Eom, S.H.; Hong, Y.H.; Lee, S.J.; Lee, H.S.; Lee, D.Y.; Pyun, Y.R. Distinct Metal Dependence for Catalytic and Structural Functions in the L-Arabinose Isomerases from the Mesophilic *Bacillus Halodurans* and the Thermophilic *Geobacillus Stearothermophilus*. *Arch. Biochem. Biophys.* **2005**, *434*, 333–343. [[CrossRef](#)]
77. Manjasetty, B.A.; Chance, M.R. Crystal Structure of *Escherichia Coli* L-Arabinose Isomerase (ECAI), The Putative Target of Biological Tagatose Production. *J. Mol. Biol.* **2006**, *360*, 297–309. [[CrossRef](#)]
78. Chouayekh, H.; Bejar, W.; Rhimi, M.; Jelleli, K.; Mseddi, M.; Bejar, S. Characterization of an L-Arabinose Isomerase from the *Lactobacillus Plantarum* NC8 Strain Showing Pronounced Stability at Acidic PH. *FEMS Microbiol. Lett.* **2007**, *277*, 260–267. [[CrossRef](#)]
79. Lee, D.W.; Jang, H.J.; Choe, E.A.; Kim, B.C.; Lee, S.J.; Kim, S.B.; Hong, Y.H.; Pyun, Y.R. Characterization of a Thermostable L-Arabinose (D-Galactose) Isomerase from the Hyperthermophilic Eubacterium *Thermotoga Maritima*. *Appl. Environ. Microbiol.* **2004**, *70*, 1397–1404. [[CrossRef](#)]
80. Zhang, Y.W.; Jeya, M.; Lee, J.K. Enhanced Activity and Stability of L-Arabinose Isomerase by Immobilization on Aminopropyl Glass. *Appl. Microbiol. Biotechnol.* **2011**, *89*, 1435–1442. [[CrossRef](#)]
81. De Sousa, M.; Manzo, R.M.; García, J.L.; Mammarella, E.J.; Gonçalves, L.R.B.; Pessela, B.C. Engineering the L-Arabinose Isomerase from *Enterococcus Faecium* for d-Tagatose Synthesis. *Molecules* **2017**, *22*, 2164. [[CrossRef](#)]
82. Cheon, J.; Kim, S.B.; Park, S.W.; Han, J.K.; Kim, P. Characterization of L-Arabinose Isomerase in *Bacillus Subtilis*, a GRAS Host, for the Production of Edible Tagatose. *Food Biotechnol.* **2009**, *23*, 8–16. [[CrossRef](#)]
83. Oh, D.K.; Kim, H.J.; Ryu, S.A.; Rho, H.J.; Kim, P. Development of an Immobilization Method of L-Arabinose Isomerase for Industrial Production of Tagatose. *Biotechnol. Lett.* **2001**, *23*, 1859–1862. [[CrossRef](#)]
84. Kim, H.J.; Oh, D.K. Purification and Characterization of an L-Arabinose Isomerase from an Isolated Strain of *Geobacillus Thermodenitrificans* Producing d-Tagatose. *J. Biotechnol.* **2005**, *120*, 162–173. [[CrossRef](#)]
85. Nguyen, T.K.; Hong, M.G.; Chang, P.S.; Lee, B.H.; Yoo, S.H. Biochemical Properties of L-Arabinose Isomerase from *Clostridium Hylemonae* to Produce D-Tagatose as a Functional Sweetener. *PLoS ONE* **2018**, *13*, e0196099. [[CrossRef](#)]
86. Siddiqui, K.S.; Ertan, H.; Poljak, A.; Bridge, W.J. Evaluating Enzymatic Productivity—The Missing Link to Enzyme Utility. *Int. J. Mol. Sci.* **2022**, *23*, 6908. [[CrossRef](#)] [[PubMed](#)]
87. Staudigl, P.; Haltrich, D.; Peterbauer, C.K. L-Arabinose Isomerase and d-Xylose Isomerase from *Lactobacillus Reuteri*: Characterization, Coexpression in the Food Grade Host *Lactobacillus Plantarum*, and Application in the Conversion of d-Galactose and d-Glucose. *J. Agric. Food Chem.* **2014**, *62*, 1617–1624. [[CrossRef](#)]
88. Prabhu, P.; Jeya, M.; Lee, J.K. Probing the Molecular Determinant for the Catalytic Efficiency of L-Arabinose Isomerase from *Bacillus Licheniformis*. *Appl. Environ. Microbiol.* **2010**, *76*, 1653–1660. [[CrossRef](#)]
89. Guo, Z.; Long, L.; Ding, S. Characterization of an L-Arabinose Isomerase from *Bacillus Velezensis* and Its Application for L-Ribulose and L-Ribose Biosynthesis. *Appl. Biochem. Biotechnol.* **2020**, *192*, 935–951. [[CrossRef](#)]

Disclaimer/Publisher’s Note: The statements, opinions and data contained in all publications are solely those of the individual author(s) and contributor(s) and not of MDPI and/or the editor(s). MDPI and/or the editor(s) disclaim responsibility for any injury to people or property resulting from any ideas, methods, instructions or products referred to in the content.